

Testing pleiotropy vs. separate QTL in multiparental populations

Frederick J. Boehm^{*}, Elissa J. Chesler[†], Brian S. Yandell^{*,‡} and Karl W. Broman^{§,1}

^{*}Department of Statistics, University of Wisconsin-Madison, Madison, Wisconsin 53706, [†]The Jackson Laboratory, Bar Harbor, Maine 04609, [‡]Department of Horticulture, University of Wisconsin-Madison, Madison, Wisconsin 53706, [§]Department of Biostatistics and Medical Informatics, University of Wisconsin-Madison, Madison, Wisconsin 53706

ABSTRACT

The high mapping resolution of multiparental populations, combined with technology to measure tens of thousands of phenotypes, presents a need for quantitative methods to enhance understanding of the genetic architecture of complex traits. When multiple traits map to a common genomic region, knowledge of the number of distinct loci provides important insight into the underlying mechanism and can assist planning for subsequent experiments. We extend the method of [Jiang and Zeng \(1995\)](#), for testing pleiotropy with a pair of traits, to the case of more than two alleles. We also incorporate polygenic random effects to account for population structure. We use a parametric bootstrap to determine statistical significance. We apply our methods to a behavioral genetics data set from Diversity Outbred mice, where we find evidence for presence of two distinct loci in a 2.5 cM region. Our methods have been incorporated into the R package `qt12pleio`.

KEYWORDS Quantitative trait locus; pleiotropy; multivariate analysis; linear mixed effects models; systems genetics

Complex trait studies in multiparental populations present new challenges in statistical methods and data analysis. Among these is the development of strategies for multivariate trait analysis. The joint analysis of two or more traits allows one to address additional questions, such as whether two traits share a single pleiotropic locus.

Previous research addressed the question of pleiotropy vs. separate QTL in two-parent crosses. [Jiang and Zeng \(1995\)](#) developed a likelihood ratio test for pleiotropy vs. separate QTL for a pair of traits. Their approach assumed that each trait was affected by a single QTL. Under the null hypothesis, the two traits were affected by a common QTL, and under the alternative hypothesis the two traits were affected by distinct QTL. [Knott and Haley \(2000\)](#) used linear regression to develop a fast approximation to the test of [Jiang and Zeng \(1995\)](#), while [Tian *et al.* \(2016\)](#) used the methods from [Knott and Haley \(2000\)](#) to dissect QTL hotspots in a F_2 population.

Multiparental populations, such as the Diversity Outbred (DO) mouse population ([Churchill *et al.* 2012](#)), enable high-precision mapping of complex traits ([de Koning and McIntyre 2014](#)). The DO mouse population began with progenitors of the Collaborative Cross (CC) mice ([Churchill *et al.* 2004](#)) Each DO mouse is a highly heterozygous genetic mosaic of alleles from the eight CC founder lines. Random matings among non-siblings have maintained the DO population for more than 23 generations ([Chesler *et al.* 2016](#)).

Several limitations of previous pleiotropy vs. separate QTL tests prevent their direct application in multiparental populations. First, multiparental populations can have complex patterns of relatedness among subjects, and failure to account for these patterns of relatedness may lead to spurious results ([Yang *et al.* 2014](#)). Second, previous tests allowed for only two founder lines ([Jiang and Zeng](#)

¹Department of Biostatistics and Medical Informatics, University of Wisconsin-Madison, 2126 Genetics-Biotechnology Center, 425 Henry Mall, Madison, WI 53706. E-mail: broman@wisc.edu

42 1995). Finally, Jiang and Zeng (1995) assumed that the null distribution of the test statistic follows a
43 chi-square distribution.

44 We developed a pleiotropy vs. separate QTL test for two traits in multiparental populations. Our
45 test builds on research that Jiang and Zeng (1995), Knott and Haley (2000), Tian *et al.* (2016), and
46 Zhou and Stephens (2014) initiated. Our innovations include the accommodation of k founder alle-
47 les per locus (compared to the traditional two founder alleles per locus) and the incorporation of
48 multivariate polygenic random effects to account for relatedness. Furthermore, we implemented a
49 parametric bootstrap test to assess statistical significance (Efron 1979; Tian *et al.* 2016).

50 Below, we describe our likelihood ratio test for pleiotropy vs. separate QTL. In simulation studies,
51 we find that it is slightly conservative, and that it has power to detect two separate loci when the
52 univariate LOD peaks are strong. We further illustrate our approach with an application to data on
53 a pair of behavior traits in a population of 261 DO mice (Logan *et al.* 2013; Recla *et al.* 2014). We find
54 modest evidence for distinct QTL in a 2.5-cM region on mouse Chromosome 8.

55 **Methods**

56 Our strategy involves first identifying two traits that map to a common genomic region. We then per-
57 form a two-dimensional, two-QTL scan over the genomic region, with each trait affected by one QTL
58 of varying position. We identify the QTL position that maximizes the likelihood under pleiotropy
59 (that is, along the diagonal where the two QTL are at a common location), and the ordered pair of
60 positions that maximizes the likelihood under the model where the two QTL are allowed to be dis-
61 tinct. The logarithm of the ratio of the two likelihoods is our test statistic. We determine statistical
62 significance with a parametric bootstrap.

63 **Data structures**

64 The data consist of three objects. The first is an n by k by m array of allele probabilities for n subjects
65 with k alleles and m marker positions on a single chromosome [derived from the observed SNP
66 genotype data by a hidden Markov model; see Broman *et al.* (2019)]. The second object is an n by 2
67 matrix of phenotype values. Each column is a phenotype and each row is a subject. The third object
68 is an n by c matrix of covariates, where each row is a subject and each column is a covariate.

69 One additional object is the genotype-derived kinship matrix, which is used in the linear mixed
70 model to account for population structure. We are focusing on a defined genomic interval, and
71 we prefer to use a kinship matrix derived by the “leave one chromosome out” (LOCO) method
72 (Yang *et al.* 2014), in which the kinship matrix is derived from the genotypes for all chromosomes
73 except the chromosome under test.

74 **Statistical Models**

75 Focusing on a pair of traits and a particular genomic region of interest, the next step is a two-
76 dimensional, two-QTL scan (Jiang and Zeng 1995). We consider two QTL with each affecting a
77 different trait, and consider all possible pairs of locations for the two QTL. For each pair of posi-
78 tions, we fit the multivariate linear mixed effects model defined in Equation 1. Note that we have
79 assumed an additive genetic model throughout our analyses, but extensions to design matrices that
80 include dominance are straightforward.

$$vec(Y) = Xvec(B) + vec(G) + vec(E) \quad (1)$$

81 where Y is the n by 2 matrix of phenotypes values; X is a $2n$ by $2(k + c)$ matrix that contains the k
82 allele probabilities for the two QTL positions and the c covariates in diagonal blocks; B is a $(k + c)$

83 by 2 matrix of allele effects and covariate effects; G is a n by 2 matrix of random effects; and E is a
84 n by 2 matrix of random errors. n is the number of mice. The ‘vec’ operator stacks columns from
85 a matrix into a single vector. For example, a 2 by 2 matrix inputted to ‘vec’ results in a vector with
86 length 4. Its first two entries are the matrix’s first column, while the third and fourth entries are the
87 matrix’s second column.

88 We also impose distributional assumptions on G and E :

$$G \sim MN_{n \times 2}(0, K, V_g) \quad (2)$$

89 and

$$E \sim MN_{n \times 2}(0, I, V_e) \quad (3)$$

90 where $MN_{n \times 2}(0, V_r, V_c)$ denotes the matrix-variate (n by 2) normal distribution with mean being the
91 n by 2 matrix with all zero entries and row covariance V_r and column covariance V_c . We assume
92 that G and E are independent.

93 **Parameter inference and log likelihood calculation**

94 Inference for parameters in multivariate linear mixed effects models is notoriously difficult and
95 can be computationally intense (Meyer 1989, 1991). Thus, we estimate V_g and V_e under the null
96 hypothesis of no QTL, and then take them as fixed and known in our two-dimensional, two-QTL
97 genome scan. We use restricted maximum likelihood methods to fit the model:

$$vec(Y) = X_0 vec(B) + vec(G) + vec(E) \quad (4)$$

98 where X_0 is a $2n$ by $2(c + 1)$ matrix whose first column of each diagonal block in X_0 has all entries
99 equal to one (for an intercept); the remaining columns are the covariates.

100 We draw on our R implementation (Boehm 2018) of the GEMMA algorithm for fitting a multivari-
101 ate linear mixed effects model with expectation-maximization (Zhou and Stephens 2014). We use
102 restricted maximum likelihood fits for the variance components V_g and V_e in subsequent calcula-
103 tions of the generalized least squares solution \hat{B} .

$$\hat{B} = (X^T \hat{\Sigma}^{-1} X)^{-1} X^T \hat{\Sigma}^{-1} vec(Y) \quad (5)$$

104 where

$$\hat{\Sigma} = \hat{V}_g \otimes K + \hat{V}_e \otimes I_n \quad (6)$$

105 where \otimes denotes the Kronecker product, K is the kinship matrix, and I_n is a n by n identity matrix.
106 We then calculate the log likelihood for a normal distribution with mean $X vec(\hat{B})$ and covariance $\hat{\Sigma}$
107 that depends on our estimates of V_g and V_e (Equation 6).

108 **Pleiotropy vs. separate QTL hypothesis testing framework**

109 Our test applies to two traits considered simultaneously. Below, λ_1 and λ_2 denote putative locus
110 positions for traits one and two. We quantitatively state the competing hypotheses for our test as:

$$\begin{aligned} H_0 : \lambda_1 &= \lambda_2 \\ H_A : \lambda_1 &\neq \lambda_2 \end{aligned} \quad (7)$$

111 Our likelihood ratio test statistic is:

$$\text{LOD} = \log_{10} \left[\frac{\max_{\lambda_1, \lambda_2} L(B, \Sigma, \lambda_1, \lambda_2)}{\max_{\lambda} L(B, \Sigma, \lambda, \lambda)} \right] \quad (8)$$

112 where L is the likelihood for fixed QTL positions, maximized over all other parameters.

113 **Visualizing profile LOD traces**

114 The output of the above analysis is a two-dimensional \log_{10} likelihood surface. To visualize these
115 results, we followed an innovation of [Zeng *et al.* \(2000\)](#) and [Tian *et al.* \(2016\)](#), and plot three traces:
116 the results along the diagonal (corresponding to the null hypothesis of pleiotropy), and then the
117 profiles derived by fixing one QTL's position and maximizing over the other QTL's position.

118 We define the LOD score for our test:

$$\text{LOD}(\lambda_1, \lambda_2) = ll_{10}(\lambda_1, \lambda_2) - \max ll_{10}(\lambda, \lambda) \quad (9)$$

119 where ll_{10} denotes \log_{10} likelihood.

120 We follow [Zeng *et al.* \(2000\)](#) and [Tian *et al.* \(2016\)](#) in defining profile LOD by the equation

$$\text{profile LOD}_1(\lambda_1) = \max_{\lambda_2} \text{LOD}(\lambda_1, \lambda_2) \quad (10)$$

121 We define profile $\text{LOD}_2(\lambda_2)$ analogously. The profile LOD_1 and profile LOD_2 traces have the same
122 maximum value, which is non-negative and gives the overall LOD test statistic.

123 We construct the pleiotropy trace by calculating the log-likelihoods for the pleiotropic models at
124 every position.

$$\text{LOD}_p(\lambda) = ll_{10}(\lambda, \lambda) - \max ll_{10}(\lambda, \lambda) \quad (11)$$

125 By definition, the maximum value for this pleiotropy trace is zero.

126 **Bootstrap for test statistic calibration**

127 We use a parametric bootstrap to determine statistical significance ([Efron 1979](#)). While [Jiang and Zeng](#)
128 [\(1995\)](#) used quantiles of a chi-squared distribution to determine p-values, this does not account
129 for the two-dimensional search over QTL positions. We follow the approach of [Tian *et al.* \(2016\)](#),
130 and identify the maximum likelihood estimate of the QTL position under the null hypothesis of
131 pleiotropy. We then use the inferred model parameters under that model and with the QTL at that
132 position to simulate bootstrap data sets according to the model in equations 1–3. For each of b boot-
133 strap data sets, we perform a two-dimensional QTL scan (over the genomic region of interest) and
134 derive the test statistic value. We treat these b test statistics as the empirical null distribution, and
135 calculate a p-value as the proportion of the b bootstrap test statistics that equal or exceed the ob-
136 served one, with the original data, $p = \#\{i : \text{LOD}_i^* \geq \text{LOD}\} / b$ where LOD_i^* denotes the LOD score
137 for the i th bootstrap replicate and LOD is the observed test statistic.

138 **Data & Software Availability**

139 Our methods have been implemented in an R package, `qt12pleio`, available at GitHub:

140 <https://github.com/fboehm/qt12pleio>

141 Custom R code for our analyses and simulations are at GitHub:

142 <https://github.com/fboehm/qt2pleio-manuscript>

143 The data from [Recla *et al.* \(2014\)](#) and [Logan *et al.* \(2013\)](#) are available at the Mouse Phenome Database:

Table 1 Type I error rates for all runs in our 2^3 experimental design. We set (marginal) genetic variances (*i.e.*, diagonal elements of V_g) to 1 in all runs. V_e was set to the 2 by 2 identity matrix in all runs. We used allele probabilities at a single genetic marker to simulate traits for all eight sets of parameter inputs. In the column “Allele effects partitioning”, “ABCD:EFGH” means that lines A–D carry one QTL allele while lines E–H carry the other allele. “F:ABCDEGH” means the QTL has a private allele in strain F.

Run	Δ (Allele effects)	Allele effects partitioning	Genetic correlation	Type I error rate
1	6	ABCD:EFGH	0	0.032
2	6	ABCD:EFGH	0.6	0.035
3	6	F:ABCDEGH	0	0.040
4	6	F:ABCDEGH	0.6	0.045
5	12	ABCD:EFGH	0	0.038
6	12	ABCD:EFGH	0.6	0.042
7	12	F:ABCDEGH	0	0.025
8	12	F:ABCDEGH	0.6	0.025

144 <https://phenome.jax.org/projects/Chesler4> and <https://phenome.jax.org/projects/Recla1>.
145 They are also available in R/qtl2 format at <https://github.com/rqtl/qtl2data>.

146 Simulation studies

147 We performed two types of simulation studies, one for type I error rate assessment and one to
148 characterize the power to detect separate QTL. To simulate traits, we specified X , B , V_g , K , and V_e
149 matrices (Equations 1–3). For both we used the allele probabilities from a single genomic region
150 derived empirically from data for a set of 479 Diversity Outbred mice from Keller *et al.* (2018).

151 Type I error rate analysis

152 To quantify type I error rate (*i.e.*, false positive rate), we simulated 400 pairs of traits for each of eight
153 sets of parameter inputs (Table 1). We used a 2^3 factorial experimental design with three factors:
154 allele effects difference, allele effects partitioning, and genetic correlation, *i.e.*, the off-diagonal entry
155 in the 2 by 2 matrix V_g .

156 We chose two strong allele effects difference values, 6 and 12. These ensured that the univariate
157 phenotypes mapped with high LOD scores to the region of interest. For the allele partitioning factor,
158 we used either equally frequent QTL alleles, or a private allele in the CAST strain (F). For the residual
159 genetic correlation (the off-diagonal entry in V_g), we considered the values 0 and 0.6. The marginal
160 genetic variances (*i.e.*, the diagonal entries in V_g) for each trait were always set to one.

161 We performed 400 simulation replicates per set of parameter inputs, and each used $b = 400$
162 bootstrap samples. For each bootstrap sample, we calculated the test statistic (Equation 8). We
163 then compared the test statistic from the simulated trait against the empirical distribution of its 400
164 bootstrap test statistics. When the simulated trait’s test statistic exceeded the 0.95 quantile of the
165 empirical distribution of bootstrap test statistics, we rejected the null hypothesis. We observed that

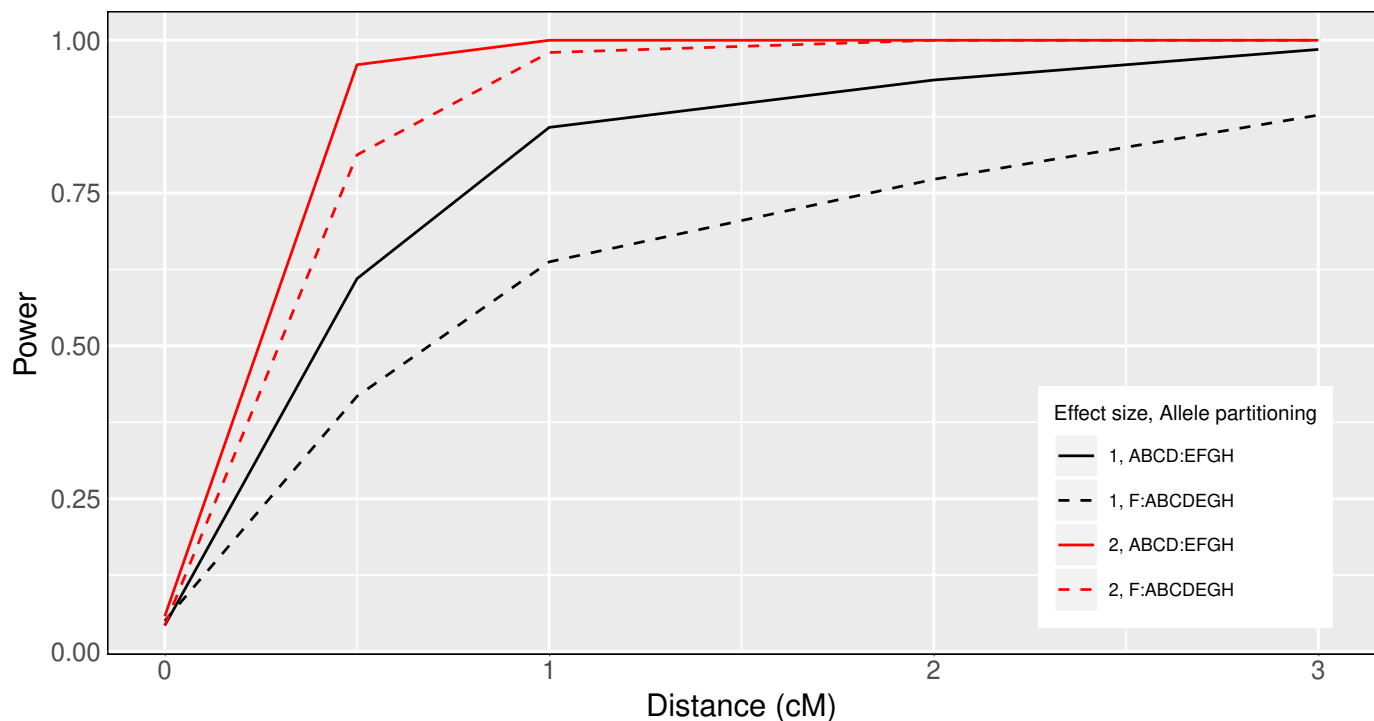


Figure 1 Pleiotropy vs. separate QTL power curves for each of four sets of parameter settings. Factors that differ among the four curves are allele effects difference and allele partitioning. Red denotes high allele effects difference, while black is the low allele effects difference. Solid line denotes the even allele partitioning (ABCD:EFGH), while dashed line denotes the uneven allele partitioning (F:ABCDEGH).

166 the test is slightly conservative over our range of parameter selections (Table 1), with estimated type
167 I error rates < 0.05 .

168 **Power analysis**

169 We also investigated the power to detect the presence of two distinct QTL. We used a $2 \times 2 \times 5$
170 experimental design, where our three factors were allele effects difference, allele effects partitioning,
171 and inter-locus distance. The two levels of allele effects difference were 1 and 2. The two levels of
172 allele effects partitioning were as in the type I error rate studies, ABCD:EFGH and F:ABCDEGH
173 (Table S1). The five levels of interlocus distance were 0, 0.5, 1, 2, and 3 cM. V_g and V_e were both set
174 to the 2 by 2 identity matrix in all power study simulations.

175 We simulated 400 pairs of traits per set of parameter inputs. For each simulation replicate, we
176 calculated the likelihood ratio test statistic. We then applied our parametric bootstrap to determine
177 the statistical significance of the results. For each simulation replicate, we used $b = 400$ bootstrap
178 samples. Because the bootstrap test statistics within a single set of parameter inputs followed ap-
179 proximately the same distribution, we pooled the $400 * 400 = 160,000$ bootstrap samples per set
180 of parameter inputs and compared each test statistic to the empirical distribution derived from the
181 160,000 bootstrap samples. However, for parameter inputs with interlocus distance equal to zero,
182 we did not pool the 160,000 bootstrap samples; instead, we proceeded by calculating power (*i.e.*,
183 type I error rate, in this case), as we did in the type I error rate study above.

184 We present our power study results in Figure 1. Power increases as interlocus distance increases.
185 The top two curves correspond to the case where the QTL effects are largest. For each value for the

186 QTL effect, power is greater when the QTL alleles are equally frequent, and smaller when a QTL
187 allele is private to one strain. One can have high power to detect that the two traits have distinct
188 QTL when they are separated by > 1 cM and when the QTL have large effect.

189 Application

190 To illustrate our methods, we applied our test to data from [Logan et al. \(2013\)](#) and [Recla et al. \(2014\)](#),
191 on 261 DO mice measured for a set of behavioral phenotypes. [Recla et al. \(2014\)](#) identified *Hydin* as
192 the gene that underlies a QTL on Chromosome 8 at 57 cM for the “hot plate latency” phenotype (a
193 measure of pain tolerance). The phenotype “percent time in light” in a light-dark box (a measure
194 of anxiety) was measured on the same set of mice ([Logan et al. 2013](#)) and also shows a QTL near
195 this location, which led us to ask whether the same locus affects both traits. The two traits show a
196 correlation of -0.15 (Figure [S1](#)).

197 QTL analysis with the LOCO method, and using sex as an additive covariate, showed multiple
198 suggestive QTL for each phenotype (Figure [S2](#); Table [S2](#)). For our investigation of pleiotropy, we
199 focused on the interval 53–64 cM on Chromosome 8. The univariate QTL results for this region are
200 shown in Figure [2](#).

201 The estimated QTL allele effects for the two traits are quite different (Figure [3](#)). With the QTL
202 placed at 55 cM, for “percent time in light”, the WSB and PWK alleles are associated with large
203 phenotypes and NOD with low phenotypes. For “hot plate latency”, on the other hand, CAST and
204 NZO show low phenotypes and NOD and PWK are near the center.

205 In applying our test for pleiotropy, we performed a two-dimensional, two-QTL scan for the pair
206 of phenotypes. With these results, we created a profile LOD plot (Figure [4](#)). The profile LOD for
207 “percent time in light” (in brown) peaks near 55 cM, as was seen in the univariate analysis. The
208 profile LOD for “hot plate latency” (in blue) peaks near 57 cM, also similar to the univariate analysis.
209 The pleiotropy trace (in gray) peaks near 55 cM.

210 The likelihood ratio test statistic for the test of pleiotropy was 1.2. Based on a parametric bootstrap
211 with 1,000 bootstrap replicates, the estimated p-value was 0.11, indicating weak evidence for distinct
212 QTL for the two traits.

213 Discussion

214 We developed a test of pleiotropy vs. separate QTL for multiparental populations, extending the
215 work of [Jiang and Zeng \(1995\)](#) for multiple alleles and with a linear mixed model to account for
216 population structure ([Kang et al. 2010](#); [Yang et al. 2014](#)). Our simulation studies indicate that the test
217 has power to detect presence of separate loci, especially when univariate trait associations are strong
218 (Figure [1](#)). Type I error rates indicate that our test is slightly conservative (Table [1](#)).

219 In the application of our method to two behavioral phenotypes in a study of 261 Diversity Out-
220 bred mice ([Recla et al. 2014](#); [Logan et al. 2013](#)), we obtained weak evidence ($p=0.11$) for the presence
221 of two distinct QTL, with one QTL (which contained the *Hydin* gene) affecting only “hot plate la-
222 tency” and a second QTL affecting “percent time in light” (Figure [4](#)).

223 Founder allele effects plots provide further evidence for the presence of two distinct loci. As
224 [Macdonald and Long \(2007\)](#) and [King et al. \(2012\)](#) have demonstrated in their analyses of multi-
225 parental *Drosophila* populations, a biallelic pleiotropic QTL would result in allele effects plots that
226 have similar patterns. While we do not know that “percent time in light” and “hot plate latency”
227 arise from biallelic QTL, the dramatic differences that we observe in allele effects patterns further
228 support the argument for two distinct loci.

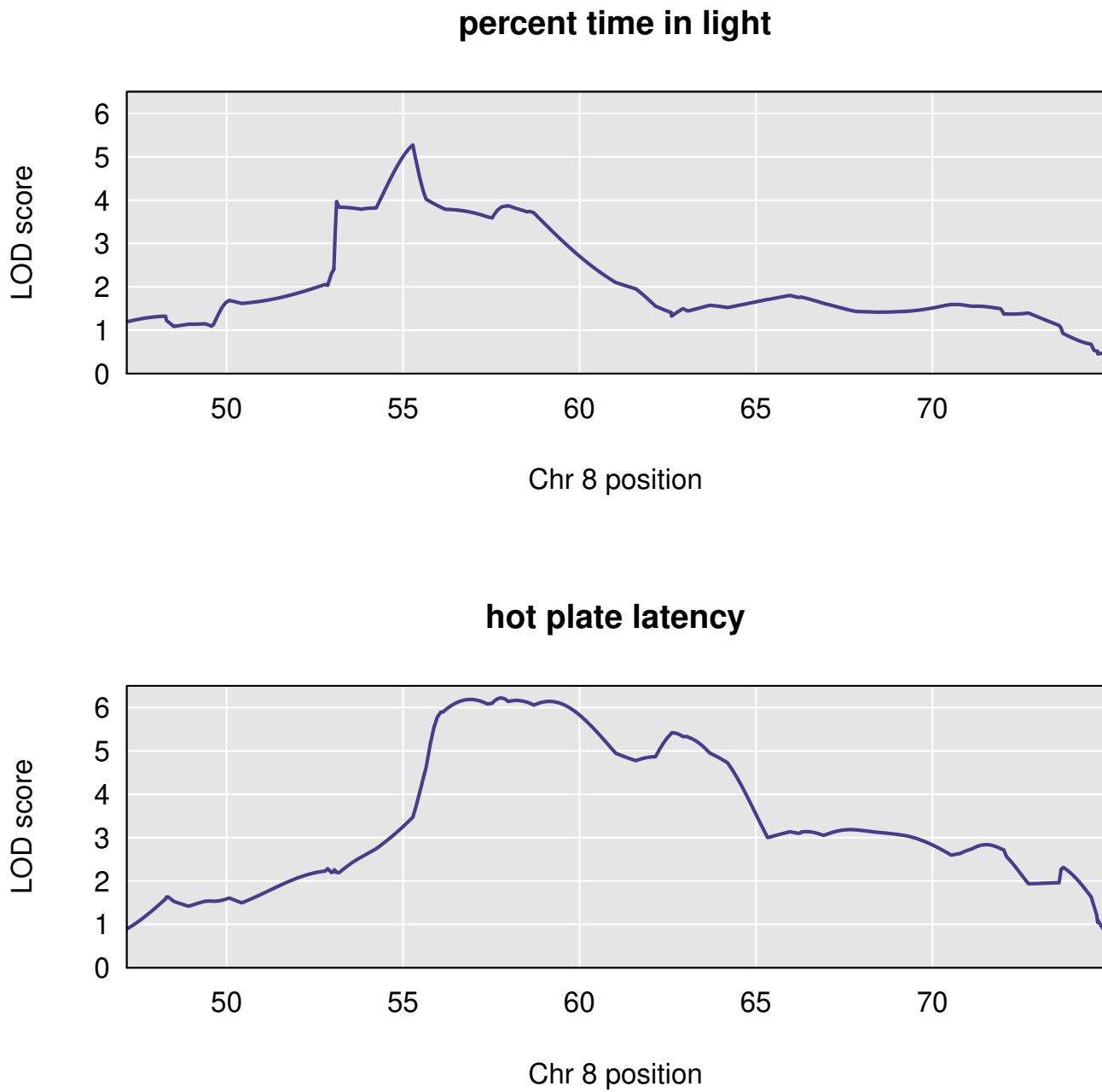


Figure 2 Chromosome 8 univariate LOD scores for percent time in light and hot plate latency reveal broad, overlapping peaks between 53 cM and 64 cM. The peak for percent time in light spans the region from approximately 53 cM to 60 cM, with a maximum near 55 cM. The peak for hot plate latency begins near 56 cM and ends about 64 cM.

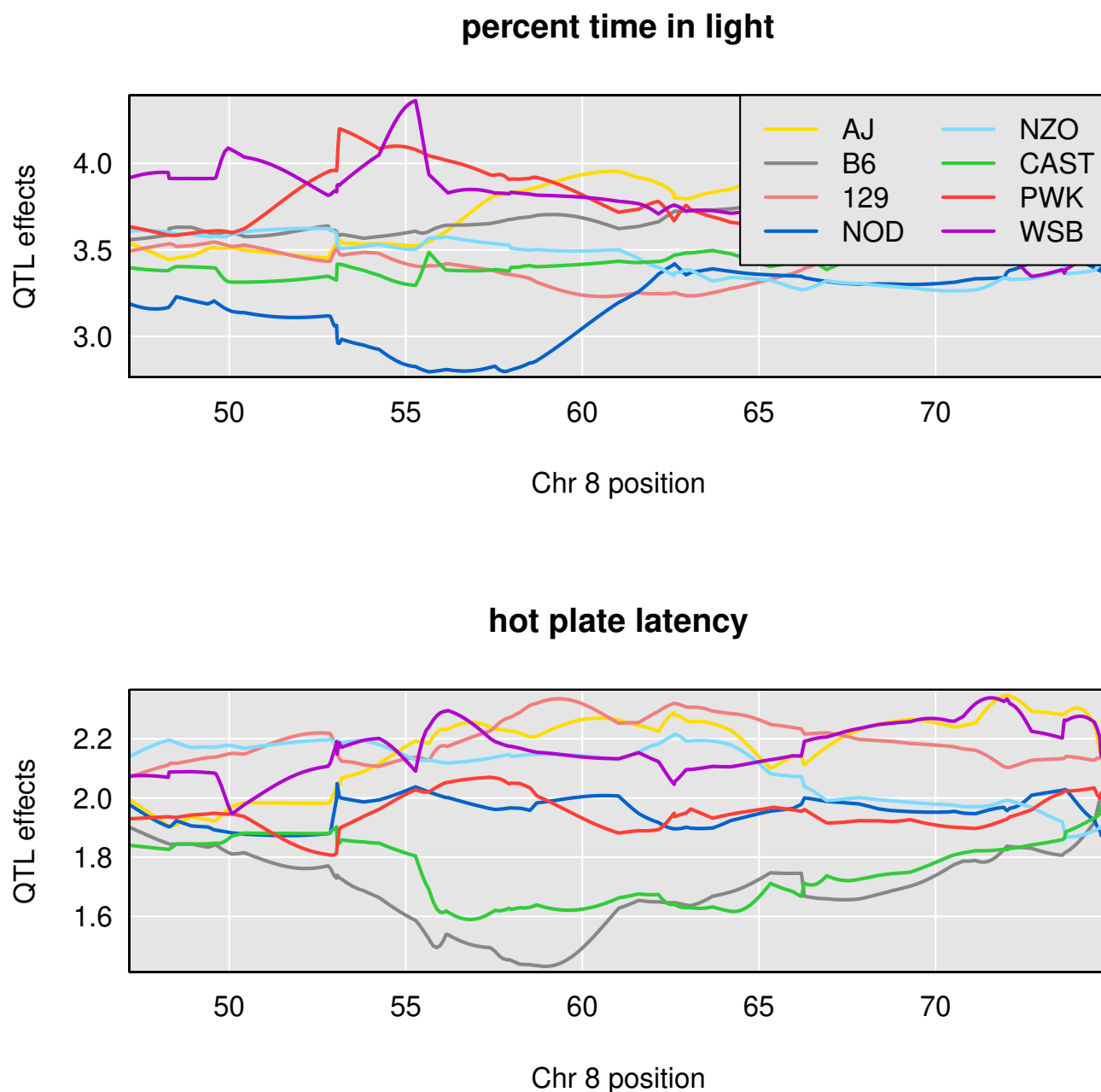


Figure 3 Chromosome 8 univariate LOD scores for percent time in light and hot plate latency reveal broad, overlapping peaks between 53 cM and 64 cM. The peak for percent time in light spans the region from approximately 53 cM to 60 cM, with a maximum near 55 cM. The peak for hot plate latency begins near 56 cM and ends about 64 cM.

percent time in light and hot plate latency

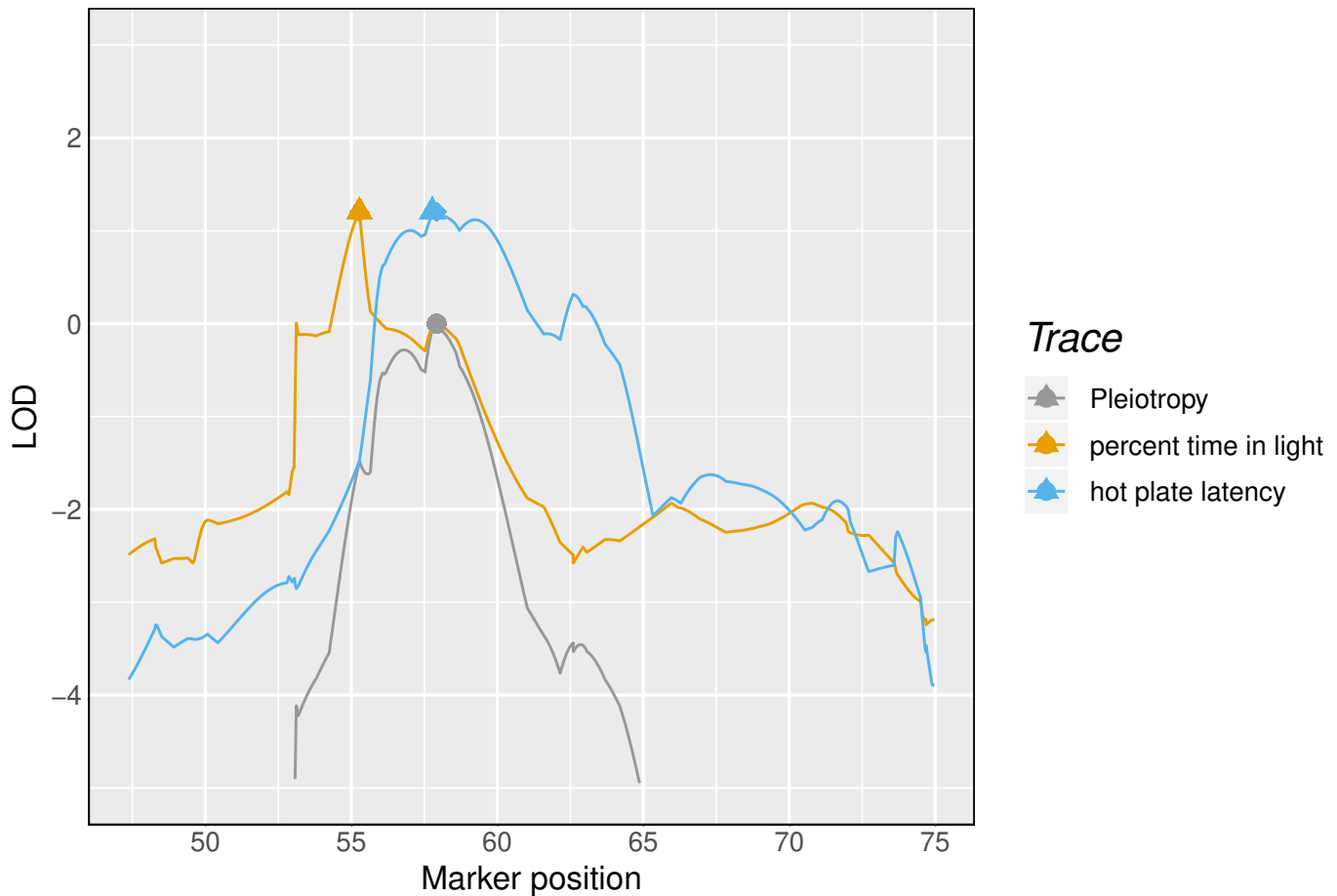


Figure 4 Profile LOD curves for the pleiotropy vs. separate QTL hypothesis test for “percent time in light” and “hot plate latency”. Gray trace denotes pleiotropy LOD values. Triangles denote the univariate LOD maxima, while diamonds denote the profile LOD maxima. For “percent time in light”, the brown triangle obscures the smaller brown diamond. Likelihood ratio test statistic value corresponds to the height of the blue and brown traces at their maxima.

229 We have implemented our methods in an R package `qt12pleio`, but analyses can be computationally intensive and time consuming. `qt12pleio` is written mostly in R, and so we could likely obtain improved computational speed by porting parts of the calculations to a compiled language such as C or C++. To accelerate our multi-dimensional QTL scans, we have integrated C++ code into `qt12pleio`, using the `Rcpp` package (Eddelbuettel *et al.* 2011).

234 Another computational bottleneck is the estimation of the variance components V_g and V_e . To accelerate this procedure, especially for the joint analysis of more than two traits, we will consider other strategies for variance component estimation, including that described by Meyer *et al.* (2018). Meyer *et al.* (2018), in joint analysis of dozens of traits, implement a bootstrap strategy to estimate variance components for lower-dimensional phenotypes before combining bootstrap estimates into valid covariance matrices for the full multivariate phenotype. Such an approach may ease some of the computational burdens that we encountered.

241 We view tests of pleiotropy as complementary to mediation tests and related methods that have become popular for inferring biomolecular causal relationships (Chick *et al.* 2016; Schadt *et al.* 2005; Baron and Kenny 1986). A mediation test proceeds by including a putative mediator as a covariate in the regression analysis of phenotype and QTL genotype; a substantial reduction in the association between genotype and phenotype corresponds to evidence of mediation.

246 Mediation analyses and our pleiotropy test ask distinct, but related, questions. Mediation analysis seeks to establish causal relationships among traits, including molecular traits, or dependent biological and behavioral processes. Pleiotropy tests examine whether two traits share a single source of genetic variation, which may act in parallel or in a causal network. Pleiotropy is required for causal relations among traits. In many cases, the pleiotropy hypothesis is the only reasonable one.

251 Schadt *et al.* (2005) argued that both pleiotropy tests and causal inference methods may contribute to gene network reconstruction. They developed a model selection strategy, based on the Akaike Information Criterion (Akaike 1974), to determine which causal model is most compatible with the observed data. Schadt *et al.* (2005) extended the methods of Jiang and Zeng (1995) to consider more complicated alternative hypotheses, such as the possibility of two QTL, one of which associates with both traits, and one of which associates with only one trait. As envisioned by Schadt *et al.* (2005), we foresee complementary roles emerging for our pleiotropy test and mediation tests in the dissection of complex trait genetic architecture.

259 Two related approaches for identifying and exploiting pleiotropy deserve mention. First, CAPE (Combined Analysis of Pleiotropy and Epistasis) is a strategy for identifying higher-order relationships among traits and marker genotypes (Tyler *et al.* 2013, 2016) and has recently been extended for use with multiparental populations, including DO mice (Tyler *et al.* 2017). CAPE exploits the pleiotropic relationship among traits in order to characterize the underlying network of QTLs, and it can suggest possible pleiotropic effects, but it does not provide an explicit test of pleiotropy. Second, Schaid *et al.* (2016) described a test for pleiotropy in the context of human genome-wide association studies (GWAS). Their approach is fundamentally different from ours, in that rather than ask whether traits are affected by a common locus or distinct loci, they ask whether the traits are all affected by a particular SNP or only some are. The difference in these approaches may be attributed to the difference in mapping resolution between human GWAS and experimental populations.

270 Technological advances in mass spectrometry and RNA sequencing have enabled the acquisition of high-dimensional biomolecular phenotypes (Ozsolak and Milos 2011; Han *et al.* 2012). Multiparental populations in *Arabidopsis*, maize, wheat, oil palm, rice, *Drosophila*, yeast, and other organisms enable high-precision QTL mapping (Yu *et al.* 2008; Tisné *et al.* 2017; Stanley *et al.* 2017; Raghavan *et al.* 2017; Mackay *et al.* 2012; Kover *et al.* 2009; Cubillos *et al.* 2013). The need to analyze high-dimensional phenotypes in multiparental populations compels the scientific community to de-

276 velop tools to study genotype-phenotype relationships and complex trait architecture. Our test, and
277 its future extensions, will contribute to these ongoing efforts.

278 **Acknowledgments**

279 The authors thank Lindsay Traeger, Julia Kemis, Qiongshi Lu, and Rene Welch for valuable sug-
280 gestions to improve the manuscript. This work was supported in part by National Institutes of
281 Health grants R01GM070683 (to K.W.B.) and P50DA039841 (to E.J.C.). The research made use of
282 compute resources and assistance of the UW-Madison Center For High Throughput Computing
283 (CHTC) in the Department of Computer Sciences at UW-Madison, which is supported by the Ad-
284 vanced Computing Initiative, the Wisconsin Alumni Research Foundation, the Wisconsin Institutes
285 for Discovery, and the National Science Foundation, and is an active member of the Open Science
286 Grid, which is supported by the National Science Foundation and the U.S. Department of Energy's
287 Office of Science.

288 **Literature Cited**

- 289 Akaike, H., 1974 A new look at the statistical model identification. *IEEE T. Automat. Contr.* **19**: 716–
290 723.
- 291 Baron, R. M. and D. A. Kenny, 1986 The moderator–mediator variable distinction in social psy-
292 chological research: Conceptual, strategic, and statistical considerations. *J. Pers. Soc. Psychol.* **51**:
293 1173–1182.
- 294 Boehm, F., 2018 *gemma2: Zhou & Stephens (2014) GEMMA multivariate linear mixed model*. R package
295 version 0.0.1.
- 296 Broman, K. W., D. M. Gatti, P. Simecek, N. A. Furlotte, P. Prins, *et al.*, 2019 R/qt12: Software for map-
297 ping quantitative trait loci with high-dimensional data and multi-parent populations. *Genetics*
298 **211**: 495–502.
- 299 Chesler, E. J., D. M. Gatti, A. P. Morgan, M. Strobel, L. Trepanier, *et al.*, 2016 Diversity outbred mice
300 at 21: Maintaining allelic variation in the face of selection. *G3* **6**: 3893–3902.
- 301 Chick, J. M., S. C. Munger, P. Simecek, E. L. Huttlin, K. Choi, *et al.*, 2016 Defining the consequences
302 of genetic variation on a proteome-wide scale. *Nature* **534**: 500–505.
- 303 Churchill, G. A., D. C. Airey, H. Allayee, J. M. Angel, A. D. Attie, *et al.*, 2004 The Collaborative Cross,
304 a community resource for the genetic analysis of complex traits. *Nat. Genet.* **36**: 1133–1137.
- 305 Churchill, G. A., D. M. Gatti, S. C. Munger, and K. L. Svenson, 2012 The diversity outbred mouse
306 population. *Mamm. Genome* **23**: 713–718.
- 307 Cubillos, F. A., L. Parts, F. Salinas, A. Bergström, E. Scovacricchi, *et al.*, 2013 High-resolution map-
308 ping of complex traits with a four-parent advanced intercross yeast population. *Genetics* **195**:
309 1141–1155.
- 310 de Koning, D.-J. and L. M. McIntyre, 2014 Genetics and G3: Community-driven science, community-
311 driven journals. *Genetics* **198**: 1–2.
- 312 Eddelbuettel, D., R. François, J. Allaire, J. Chambers, D. Bates, *et al.*, 2011 Rcpp: Seamless R and C++
313 integration. *J. Stat. Softw.* **40**: 1–18.
- 314 Efron, B., 1979 Bootstrap methods: another look at the jackknife. *Ann. Stat.* **7**: 1–26.
- 315 Han, X., K. Yang, and R. W. Gross, 2012 Multi-dimensional mass spectrometry-based shotgun
316 lipidomics and novel strategies for lipidomic analyses. *Mass Spectrom. Rev.* **31**: 134–178.
- 317 Jiang, C. and Z.-B. Zeng, 1995 Multiple trait analysis of genetic mapping for quantitative trait loci.
318 *Genetics* **140**: 1111–1127.
- 319 Kang, H. M., J. H. Sul, S. K. Service, N. A. Zaitlen, S.-y. Kong, *et al.*, 2010 Variance component model
320 to account for sample structure in genome-wide association studies. *Nat. Genet.* **42**: 348–354.

- 321 Keller, M. P., D. M. Gatti, K. L. Schueler, M. E. Rabaglia, D. S. Stapleton, *et al.*, 2018 Genetic drivers
322 of pancreatic islet function. *Genetics* **209**: 335–356.
- 323 King, E. G., C. M. Merkes, C. L. McNeil, S. R. Hoofer, S. Sen, *et al.*, 2012 Genetic dissection of a model
324 complex trait using the *Drosophila* Synthetic Population Resource. *Genome Res.* **22**: 1558–1566.
- 325 Knott, S. A. and C. S. Haley, 2000 Multitrait least squares for quantitative trait loci detection. *Genet-*
326 *ics* **156**: 899–911.
- 327 Kover, P. X., W. Valdar, J. Trakalo, N. Scarcelli, I. M. Ehrenreich, *et al.*, 2009 A multiparent ad-
328 vanced generation inter-cross to fine-map quantitative traits in *Arabidopsis thaliana*. *PLoS Genet.* **5**:
329 e1000551.
- 330 Logan, R. W., R. F. Robledo, J. M. Recla, V. M. Philip, J. A. Bubier, *et al.*, 2013 High-precision genetic
331 mapping of behavioral traits in the diversity outbred mouse population. *Genes Brain Behav.* **12**:
332 424–437.
- 333 Macdonald, S. J. and A. D. Long, 2007 Joint estimates of QTL effect and frequency using synthetic
334 recombinant populations of *Drosophila melanogaster*. *Genetics* **176**: 1261–1281.
- 335 Mackay, T. F., S. Richards, E. A. Stone, A. Barbadilla, J. F. Ayroles, *et al.*, 2012 The *Drosophila*
336 *melanogaster* genetic reference panel. *Nature* **482**: 173–178.
- 337 Meyer, H. V., F. P. Casale, O. Stegle, and E. Birney, 2018 LiMMBo: a simple, scalable ap-
338 proach for linear mixed models in high-dimensional genetic association studies. bioRxiv. DOI:
339 <https://doi.org/10.1101/255497>.
- 340 Meyer, K., 1989 Restricted maximum likelihood to estimate variance components for animal models
341 with several random effects using a derivative-free algorithm. *Genet. Sel. Evol.* **21**: 317–340.
- 342 Meyer, K., 1991 Estimating variances and covariances for multivariate animal models by restricted
343 maximum likelihood. *Genet. Sel. Evol.* **23**: 67–83.
- 344 Oszolak, F. and P. M. Milos, 2011 RNA sequencing: advances, challenges and opportunities. *Nat.*
345 *Rev. Genet.* **12**: 87–98.
- 346 Raghavan, C., R. Mauleon, V. Lacorte, M. Jubay, H. Zaw, *et al.*, 2017 Approaches in characterizing
347 genetic structure and mapping in a rice multiparental population. *G3* **7**: 1721–1730.
- 348 Recla, J. M., R. F. Robledo, D. M. Gatti, C. J. Bult, G. A. Churchill, *et al.*, 2014 Precise genetic map-
349 ping and integrative bioinformatics in Diversity Outbred mice reveals *Hydin* as a novel pain gene.
350 *Mamm. Genome* **25**: 211–222.
- 351 Schadt, E. E., J. Lamb, X. Yang, J. Zhu, S. Edwards, *et al.*, 2005 An integrative genomics approach to
352 infer causal associations between gene expression and disease. *Nat. Genet.* **37**: 710–717.
- 353 Schaid, D. J., X. Tong, B. Larrabee, R. B. Kennedy, G. A. Poland, *et al.*, 2016 Statistical methods for
354 testing genetic pleiotropy. *Genetics* **204**: 483–497.
- 355 Stanley, P. D., E. Ng’oma, S. O’Day, and E. G. King, 2017 Genetic dissection of nutrition-induced
356 plasticity in insulin/insulin-like growth factor signaling and median life span in a *Drosophila*
357 multiparent population. *Genetics* **206**: 587–602.
- 358 Tian, J., M. P. Keller, A. T. Broman, C. Kendzioriski, B. S. Yandell, *et al.*, 2016 The dissection of expres-
359 sion quantitative trait locus hotspots. *Genetics* **202**: 1563–1574.
- 360 Tisné, S., V. Pomiès, V. Riou, I. Syahputra, B. Cochard, *et al.*, 2017 Identification of ganoderma disease
361 resistance loci using natural field infection of an oil palm multiparental population. *G3* **7**: 1683–
362 1692.
- 363 Tyler, A. L., L. R. Donahue, G. A. Churchill, and G. W. Carter, 2016 Weak epistasis generally stabi-
364 lizes phenotypes in a mouse intercross. *PLoS Genet.* **12**: e1005805.
- 365 Tyler, A. L., B. Ji, D. M. Gatti, S. C. Munger, G. A. Churchill, *et al.*, 2017 Epistatic networks jointly
366 influence phenotypes related to metabolic disease and gene expression in diversity outbred mice.
367 *Genetics* **206**: 621–639.

- 368 Tyler, A. L., W. Lu, J. J. Hendrick, V. M. Philip, and G. W. Carter, 2013 CAPE: an R package for
369 combined analysis of pleiotropy and epistasis. *PLoS Comput. Biol.* **9**: e1003270.
- 370 Yang, J., N. A. Zaitlen, M. E. Goddard, P. M. Visscher, and A. L. Price, 2014 Advantages and pitfalls
371 in the application of mixed-model association methods. *Nat. Genet.* **46**: 100–106.
- 372 Yu, J., J. B. Holland, M. D. McMullen, and E. S. Buckler, 2008 Genetic design and statistical power of
373 nested association mapping in maize. *Genetics* **178**: 539–551.
- 374 Zeng, Z.-B., J. Liu, L. F. Stam, C.-H. Kao, J. M. Mercer, *et al.*, 2000 Genetic architecture of a morpho-
375 logical shape difference between two *Drosophila* species. *Genetics* **154**: 299–310.
- 376 Zhou, X. and M. Stephens, 2014 Efficient multivariate linear mixed model algorithms for genome-
377 wide association studies. *Nat. Methods* **11**: 407–409.

Table S1 Eight founder lines and their one-letter abbreviations.

Founder allele	One-letter abbreviation
A/J	A
C57BL/6J	B
129S1/SvImJ	C
NOD/ShiLtJ	D
NZO/H1LTJ	E
Cast/EiJ	F
PWK/PhJ	G
WSB/EiJ	H

Table S2 Both “hot plate latency” and “percent time in light” demonstrate multiple QTL peaks with LOD scores above 5.

phenotype	chr	pos	LOD score
percent time in light	8	55.28	5.27
hot plate latency	8	57.77	6.22
percent time in light	9	36.70	5.42
hot plate latency	9	46.85	5.22
percent time in light	11	63.39	6.46
hot plate latency	12	43.52	5.13
percent time in light	15	15.24	5.67
hot plate latency	19	47.80	5.48

hot plate latency vs. percent time in light

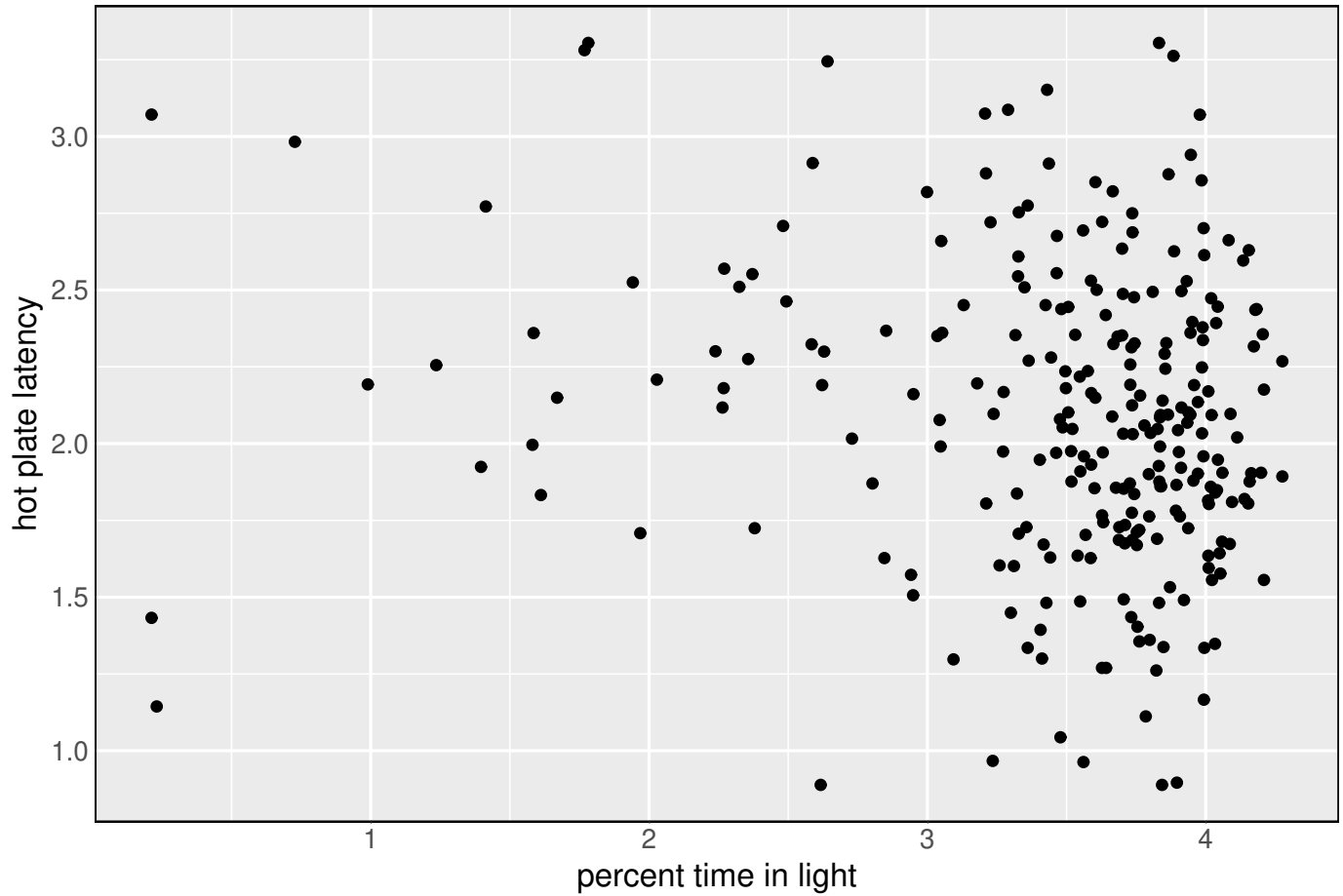


Figure S1 Scatter plot of “hot plate latency” against “percent time in light”, after applying logarithm transformations and winsorizing both traits.

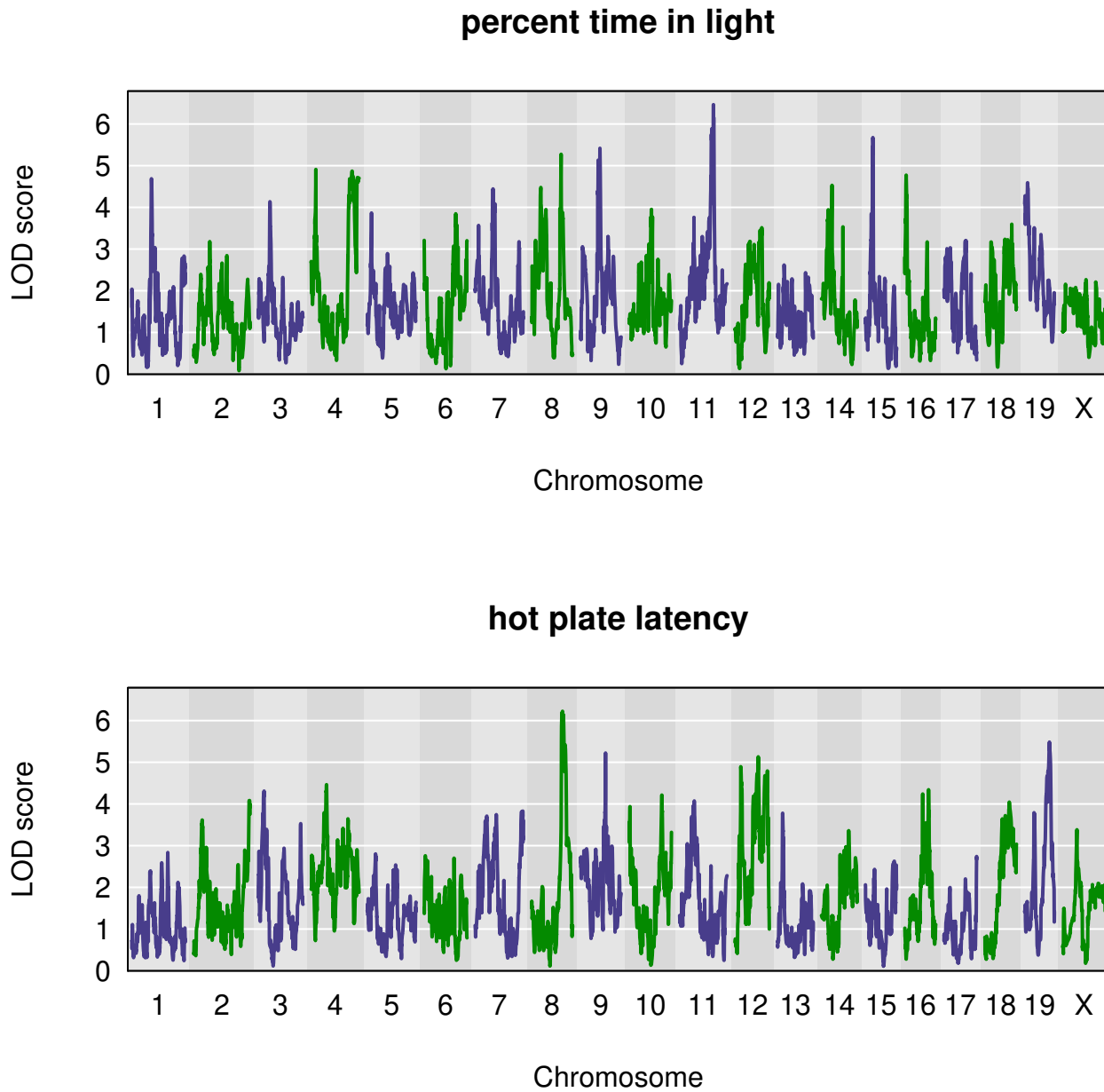


Figure S2 Genome-wide QTL scan for percent time in light reveals multiple QTL, including one on Chromosome 8.